SUPPLEMENTAL FIGURE LEGENDS

Supplemental Figure 1. Inactivation of Pten and Trp53 in Keratin 5 expressing cells does not result in bladder cancer. A) Schema showing differential expression of *Upk3a* and *Krt5* (K5) in umbrella/intermediate and basal cells of the urothelium respectively as well as the inactivation of Pten and Trp53 in the luminal and basal cell layers using *Upk3a-Cre^{ERT2}* and *K5-Cre^{ERT2}.* **B)** Kaplan-Meier survival plot of *KPPT (Krt5-Cre^{ERT2}; Pten$^{L/L}$; Trp53$^{L/L}$; Rosa26$^{LSL\text{-}tdTomato}$* mice dosed with tamoxifen by gavage or 4-hydroxytamoxifen (4-OHT) intravesicaly. **C)** Photos demonstrating the epithelial hyperplasia around the snout and skin papillomas in *KPPT* mice after dosing with tamoxifen by gavage or 4-hydroxytamoxifen intravesicaly. **D)** *KPPT* mice imaged by IVIS for tdTomato activity after the indicated treatments. **E)** Representative histology of the urothelium of a mouse 50 weeks after instillation of 200nM 4-OHT.

Supplemental Figure 2. Histologic features of BBN induced tumors. A) representative BBN tumor. **B)** squamous differentiation. **C)** lamina propria invasion. **D)** muscularis propria invasion.

Supplemental Figure 3. Generation of KT normal urothelial cells and comparison to MB49 and 3T3 cells. A) *K5^{CreERT2}; Rosa26$^{LSL\text{-}tdTomato}$* mice were dosed with tamoxifen by gavage. 7 days later mice were sacrificed, bladders homogenized and plated on 3T3J2 feeder cells. Brightfield and fluorescent images demonstrate an island of epithelial cells surrounded by fibroblasts. The epithelial cells express tdTomato

suggesting that they have expressed Krt5 resulting in conditional expression of tdTomato. **B)** Pearson correlation between UNC MB49 and FCCC MB49 cells demonstrating a high level of transcriptome correlation across all genes, R = 0.94. **C)** Hierarchical clustering of MB49 cells with 3T3 cells, our three primary mouse (KAT) urothelial cell lines, BBN963 cells, and UPPL1541 cells demonstrated that the MB49 cells co-clustered with 3T3 cells. **D)** PVClust dendrogram demonstrating that both UNC MB49 and FCCC MB49 cells co-cluster significantly with 3T3 cells rather than KAT cells (p=0.0).

Supplemental Figure 4. Hierarchical clustering of MB49, BBN963, and UPPL1541 cell lines and cell line derived tumors. A) PvClust dendrogram demonstrating that BBN963, UPPL1541, and KT normal mouse urothelial cells co-cluster 100 out of 100 times and cluster away from MB49 cells 100 out of 100 times. **B)** PvClust dendrogram demonstrating that BBN963, UPPL1541 cell line derived tumors co-cluster 100 out of 100 times and cluster away from MB49 cell line derived tumors 100 out of 100 times.

Supplemental Figure 5. IPA Pathways enriched in BBN963 versus UPPL1541 cell line derived tumors. Ingenuity Pathway Analysis was performed comparing BBN963 to UPPL1541 cell line derived tumors.

Supplemental Figure 6. MB49 cell line derived tumors are more mesenchymal than BBN963 and UPPL1541 cell line derived tumors. Boxplots indicating the RNA

expression of EMT markers *Vim* and *Cdh1* in BBN963, MB49, and UPPL1541 cell line derived tumors

Supplemental Figure 7. Immune Gene Signatures and correlation between tumor-infiltrating lymphocyte phenotype and tumor size. **A)** Heatmap of z scores of immune gene signatures from Figure 4A annotated with primary BBN and UPPL tumor name as well as immune gene signature names. **B)** Univariable correlation of tumor size to flow cytometric phenotyping in BBN963 (left) and UPPL1541 (right) tumors. Colors demonstrate positive (red) and negative (blue) correlation, with color intensity representing the degree of significance.

Supplemental Figure 8. TCR clonotype in anti-PD-1 treated BBN963 tumors. Receptor clonotype sharing of tumor infiltrating T cell receptor beta chain expression in anti-PD-1 treated responder and nonresponder BBN963 tumors, displayed as heatmap **A)** and quantification **B)**. **C)** Shannon entropy index of tumor infiltrating T cell receptor beta chain expression in anti-PD-1 treated responder and nonresponder BBN963 tumors.

Supplemental Figure 9. Memory T cell gene signature expression in TCGA BLCA tumors. Expression of effector memory T cell immune gene signatures in TGA-BLCA dataset, split by basal, luminal, and molecular claudin-low subtype.

Supplemental Figure 10. Oncoprint of whole exome sequencing of UPPL1541, BBN963, and MB49 cell line derived tumors. Cell line derived tumors from the indicated bladder cancer mouse models were subjected to whole exome sequencing. Oncoprint is shown.

Supplemental Figure 1

A

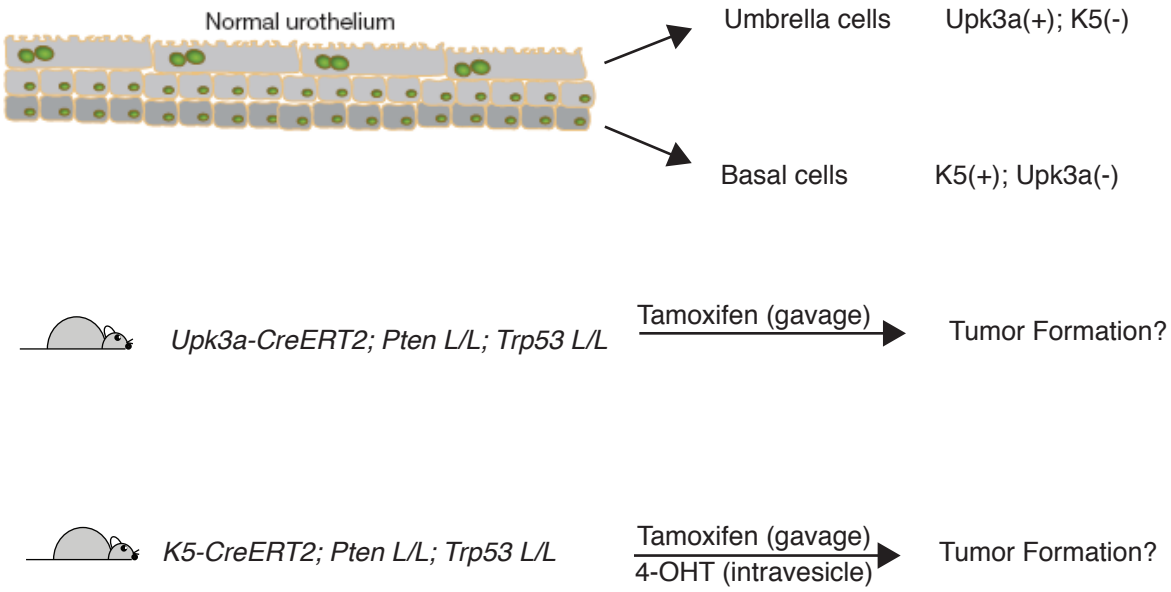

B

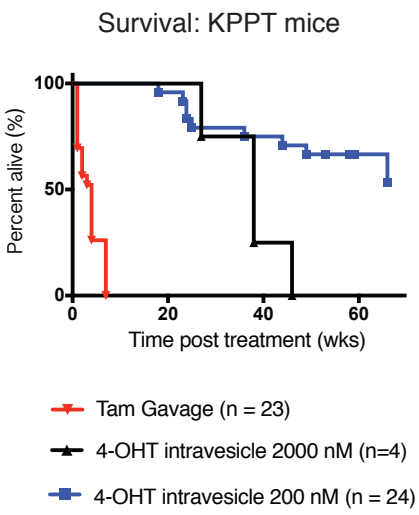

C

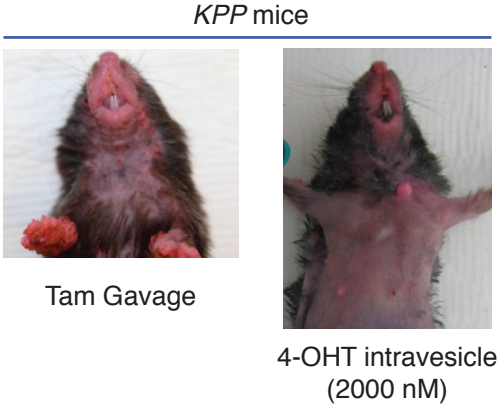

D

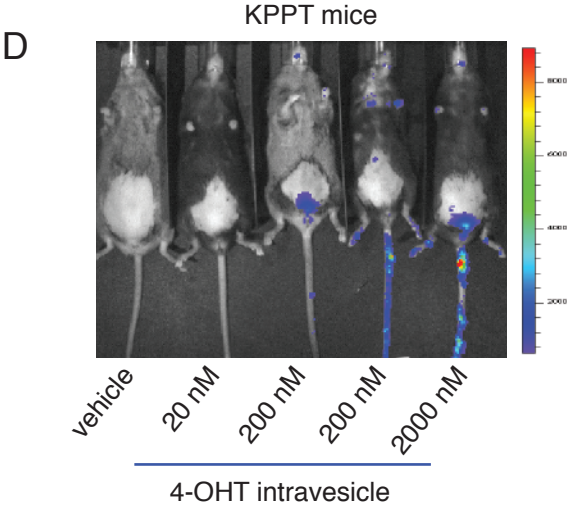

E

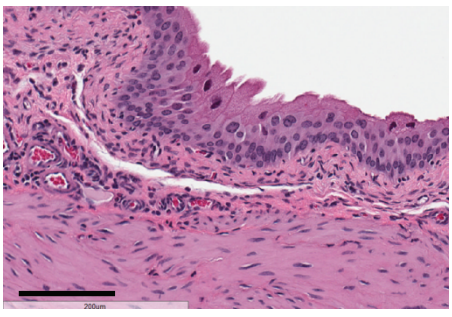

Supplemental Figure 2

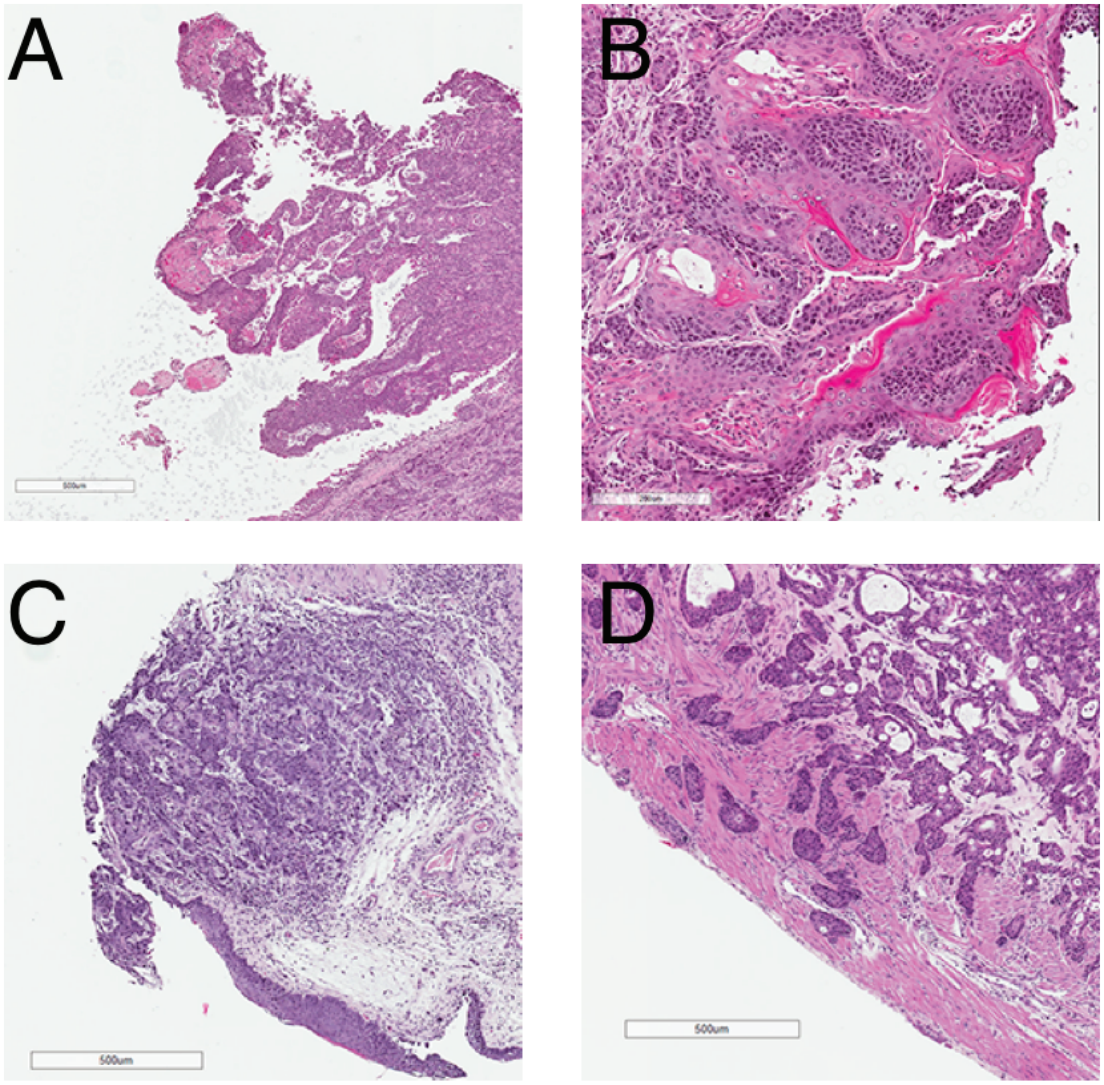

Supplemental Figure 3

A

CRC Culture: *K5Cre-ERT2; Rosa26-LSL-TdTomato*

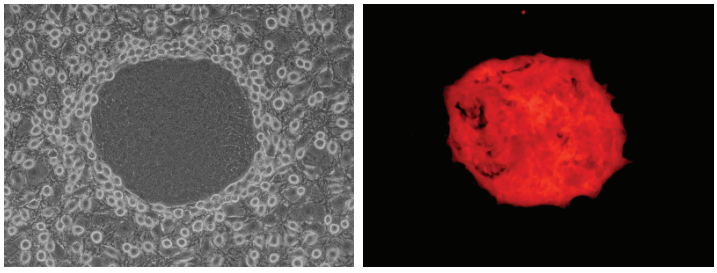

Brightfield TdTomato

B

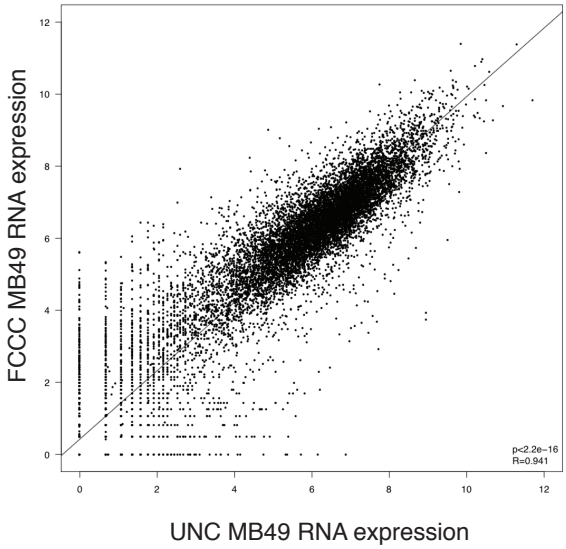

C

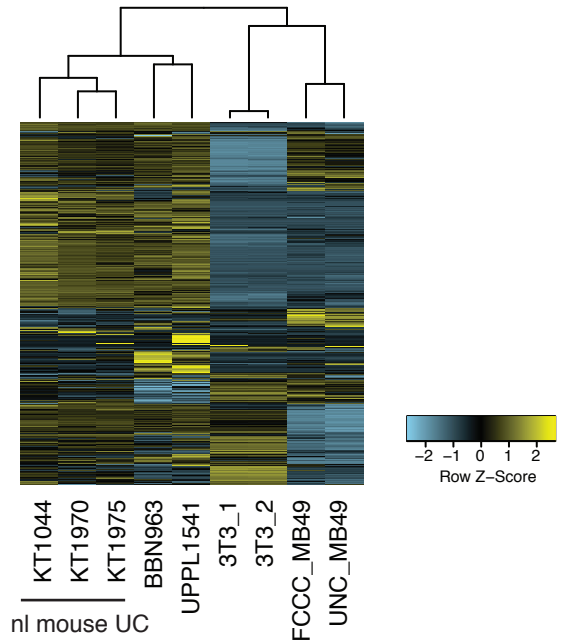

D

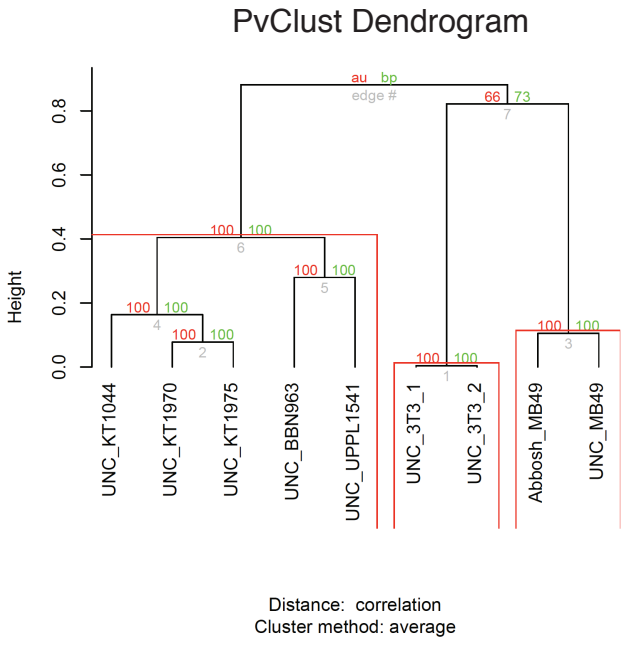

Supplemental Figure 4

A

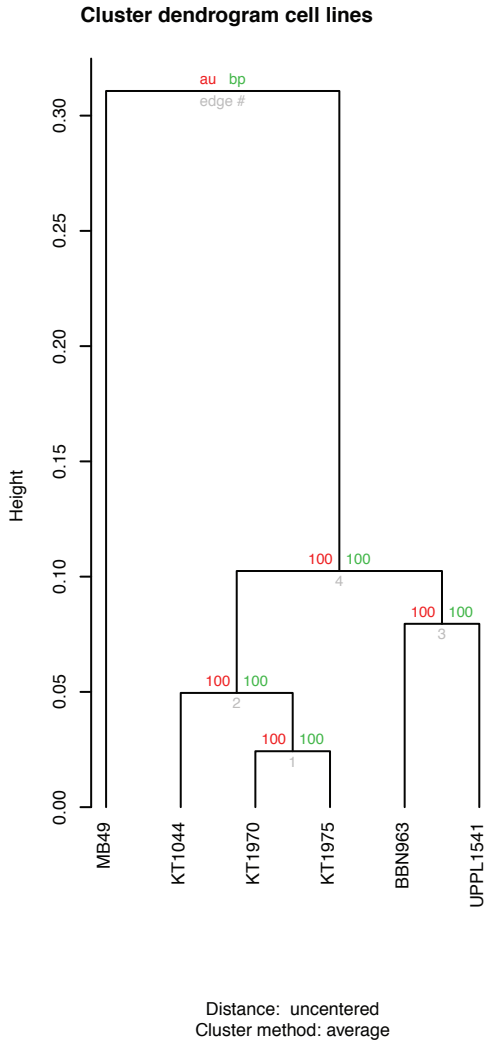

B

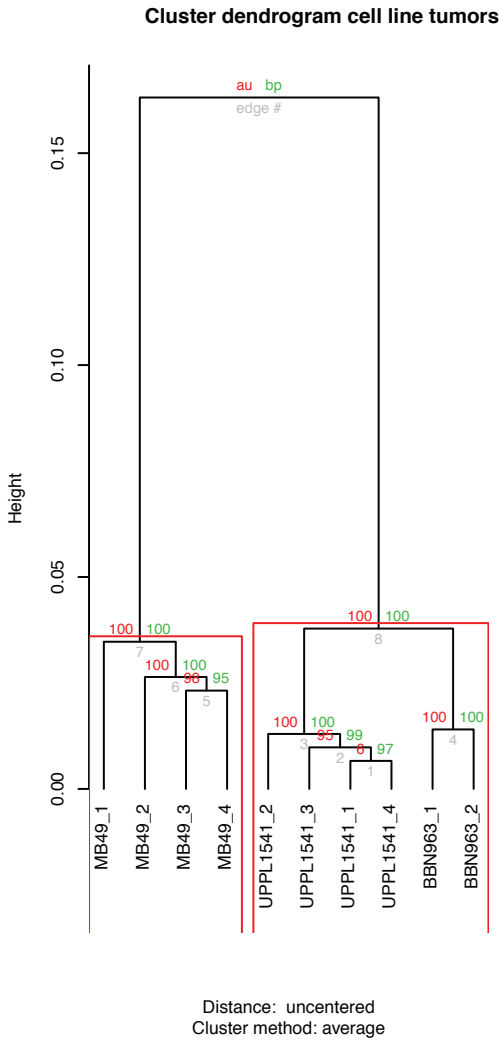

Supplemental Figure 5

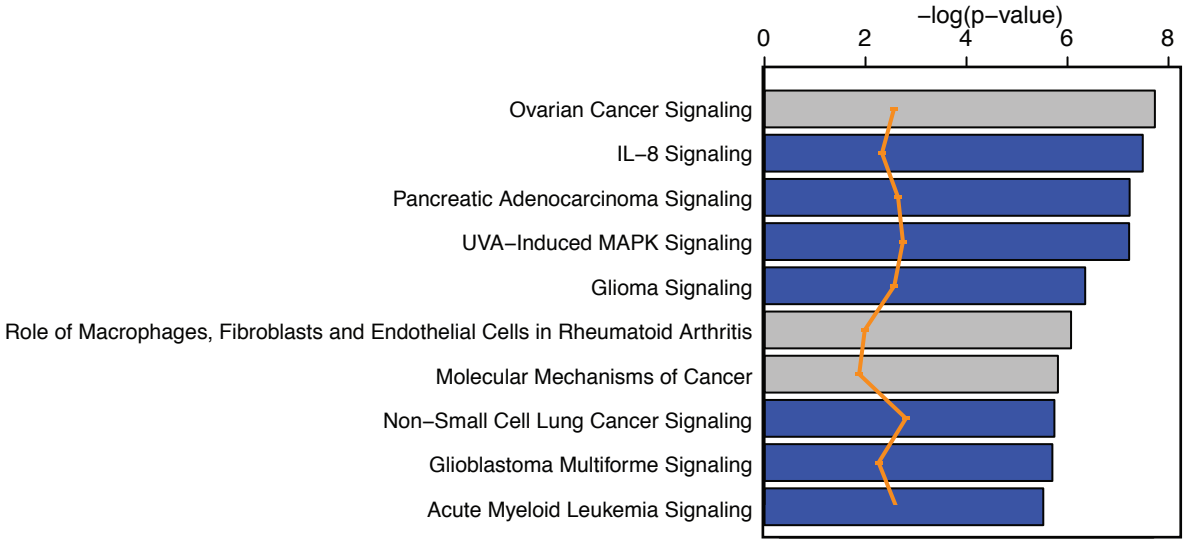

Supplemental Figure 6

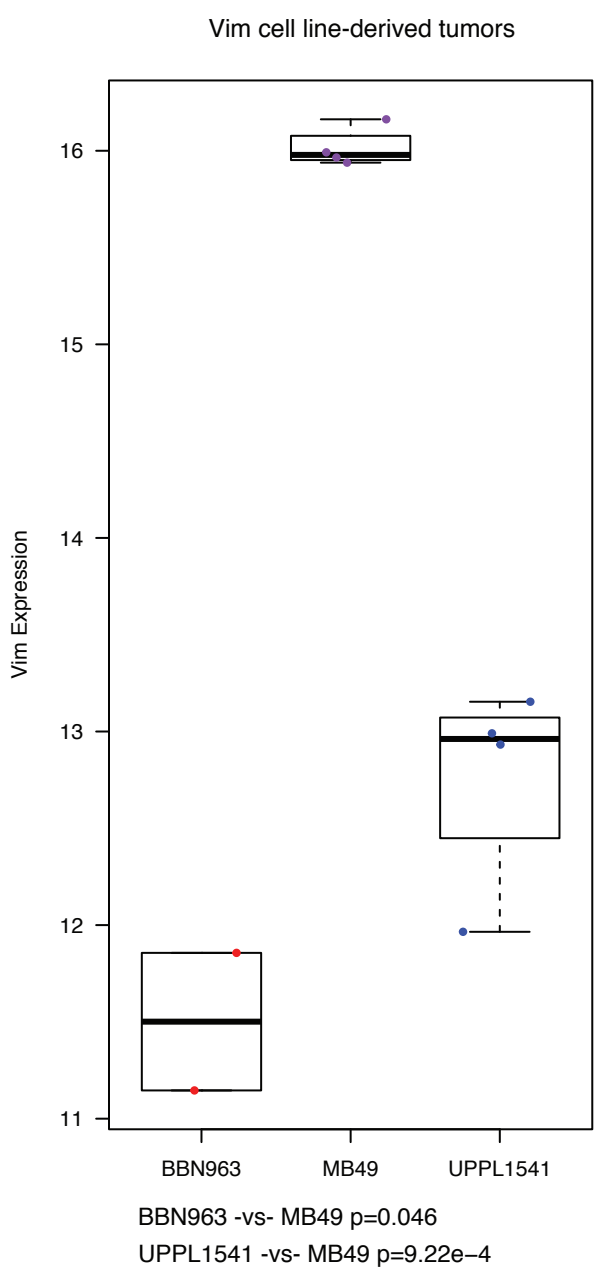

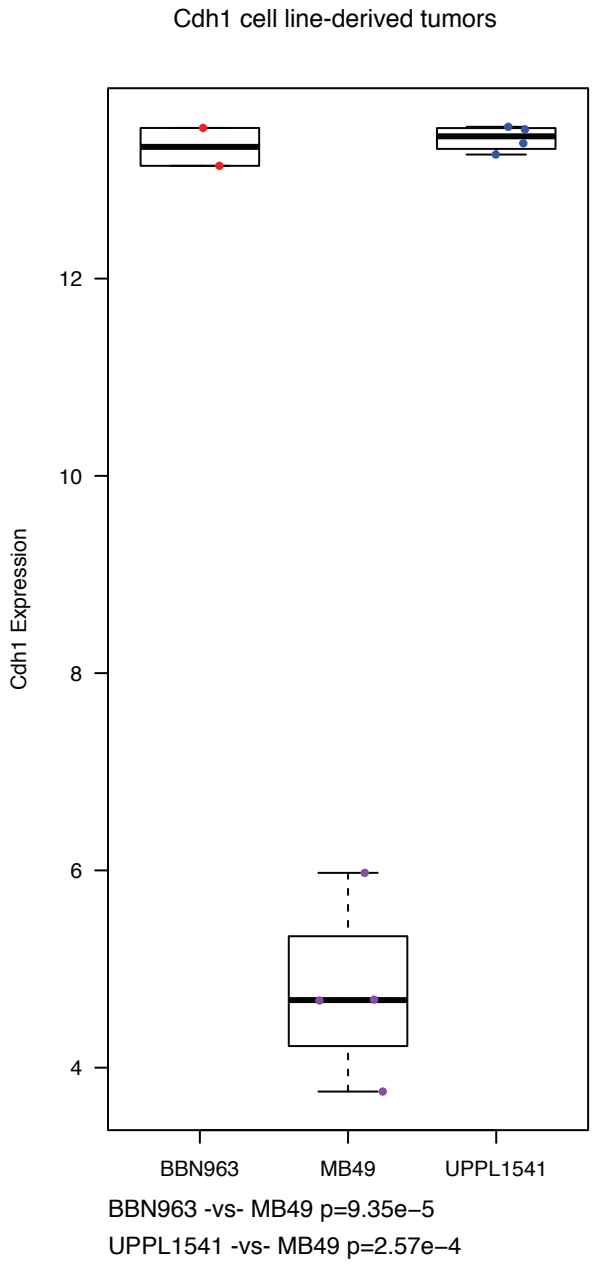

Supplemental Figure 7

A

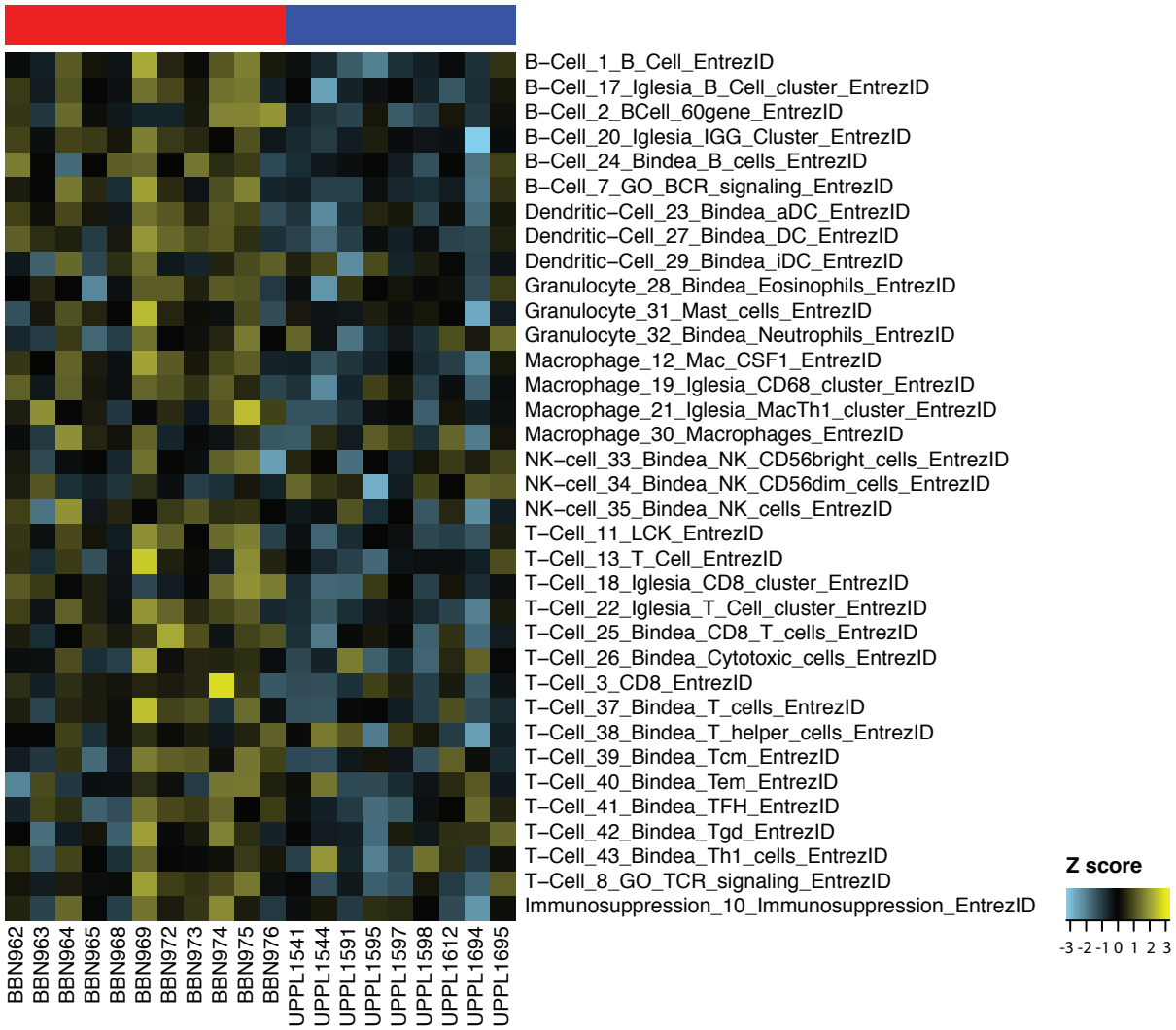

B

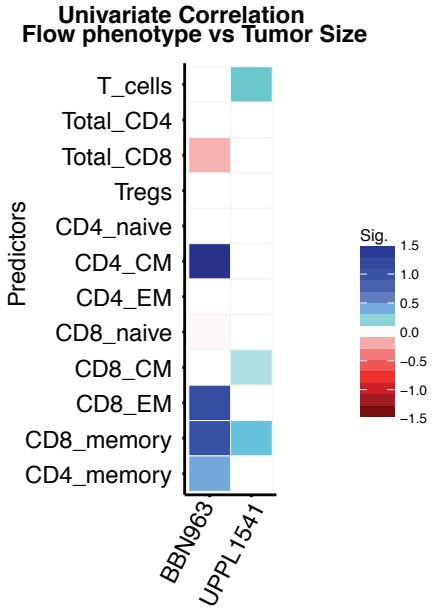

Supplemental Figure 8

A

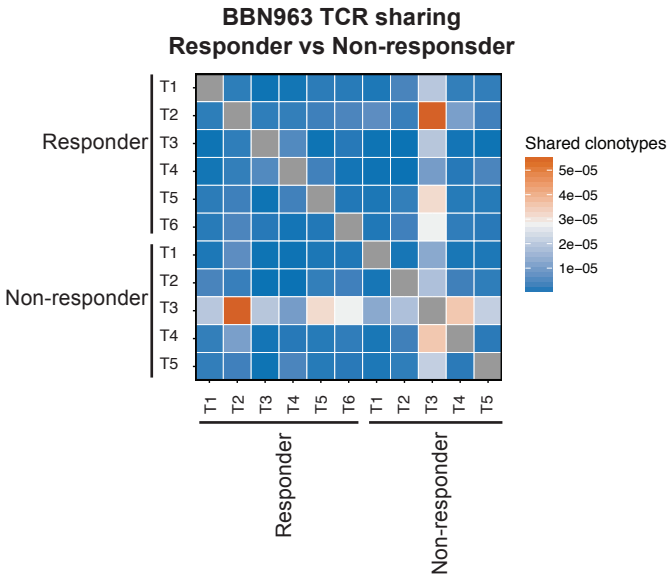

B

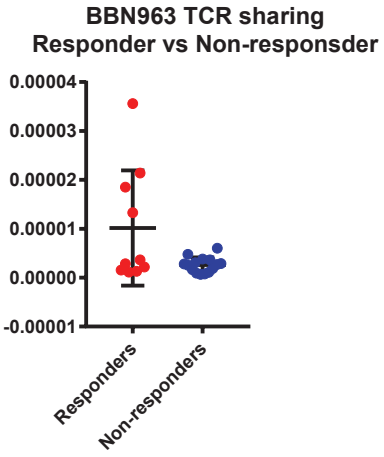

C

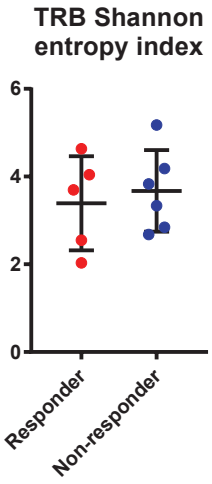

Supplemental Figure 9

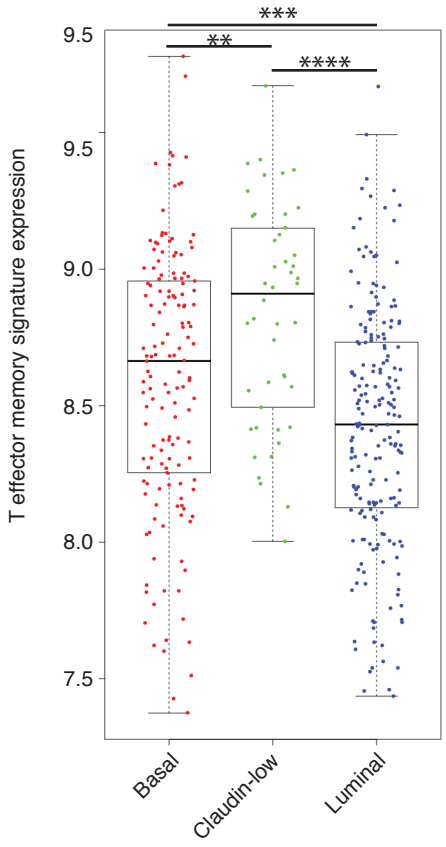

Supplemental Figure 10